First Staging of Two Laser Accelerators

W. D. Kimura,[1,*] A. van Steenbergen,[2] M. Babzien,[2] I. Ben-Zvi,[2] L. P. Campbell,[1] D. B. Cline,[3] C. E. Dilley,[1]
J. C. Gallardo,[2] S. C. Gottschalk,[1] P. He,[3] K. P. Kusche,[2] Y. Liu,[3] R. H. Pantell,[4] I. V. Pogorelsky,[3] D. C. Quimby,[1]
J. Skaritka,[2] L. C. Steinhauer,[5] and V. Yakimenko[2]

[1]*STI Optronics, Inc., Bellevue, Washington 98004*
[2]*Brookhaven National Laboratory, Upton, New York 11973*
[3]*University of California–Los Angeles, Los Angeles, California 90095*
[4]*Stanford University, Stanford, California 94305*
[5]*University of Washington, Redmond Plasma Physics Laboratory, Redmond, Washington 98052*
(Received 9 November 2000; revised manuscript received 15 March 2001)

Staging of two laser-driven, relativistic electron accelerators has been demonstrated for the first time in a proof-of-principle experiment, whereby two distinct and serial laser accelerators acted on an electron beam in a coherently cumulative manner. Output from a CO_2 laser was split into two beams to drive two inverse free electron lasers (IFEL) separated by 2.3 m. The first IFEL served to bunch the electrons into ~ 3 fs microbunches, which were rephased with the laser wave in the second IFEL. This represents a crucial step towards the development of practical laser-driven electron accelerators.

Conventional microwave electron accelerators are reaching their maximum acceleration gradient limits (~ 100 MeV/m). Higher gradients are needed for future >1-TeV accelerators for high-energy physics [1], and to enable compact, less expensive $\sim 0.1 - 1$-GeV accelerators for medical [2], materials research [3], and industrial processing [4] applications. The high fields from lasers are very attractive for acceleration; however, practical laser-driven accelerator systems will require the following: (i) grouping the electrons into microbunches much shorter than the driver wavelength (e.g., $\sim$fs); (ii) repeatedly accelerating the microbunches over many stages; and (iii) femtosecond-accurate phasing of the driver field with the microbunches at each stage. These microbunch lengths and phasing requirements are several orders of magnitude smaller than in microwave accelerators. Laser accelerators have demonstrated gradients >100 GeV/m [5], but only over several millimeter distances and not with microbunches. In a proof-of-principle experiment, we operated two laser accelerators in series for the first time and have been the first to demonstrate a system configuration that satisfies all three requirements. Our femtosecond phase control also displays a notable degree of stability without usage of active phase control.

The experiment, called STELLA (staged electron laser acceleration), was operated at the Brookhaven National Laboratory Accelerator Test Facility (ATF). This facility features a photocathode-driven, microwave linear accelerator and a high-peak power CO_2 laser [6] ($\lambda = 10.6$ μm). The experiment is briefly described here; further details can be found elsewhere [7,8].

While various laser accelerators could be used, for convenience we decided to use two identical inverse free electron lasers (IFEL) [9] for our laser accelerators. In a IFEL, a laser beam interacts with electrons traveling through a periodic magnet array called an undulator. The electrons take oscillatory trajectories through the undulator, thereby introducing a transverse velocity component in the same direction as the laser field whose linear polarization is in the plane of the electron undulations. At the proper resonance condition, the electrons stay synchronized in phase with the laser electromagnetic wave and can continuously acquire energy from the laser field.

The two IFELs are staged in series along the beam line as shown schematically in Fig. 1. Quadrupole magnets are located before each IFEL to focus the electron beam (*e*-beam) into the undulators. The STELLA undulators, manufactured by STI Optronics, use a planar array of uniformly spaced permanent magnets with a magnet period of 3.3 cm and a total undulator length of 33 cm. The pulsed CO_2 laser beam is split into two beams and sent to the IFELs. An optical delay stage permits phase adjustment of the laser beam with respect to the electrons at the entrance to the second IFEL.

The laser beams are converted to annular beams using axicon lenses (not shown). This is done in order to reflect the laser beams off mirrors inside the beam line
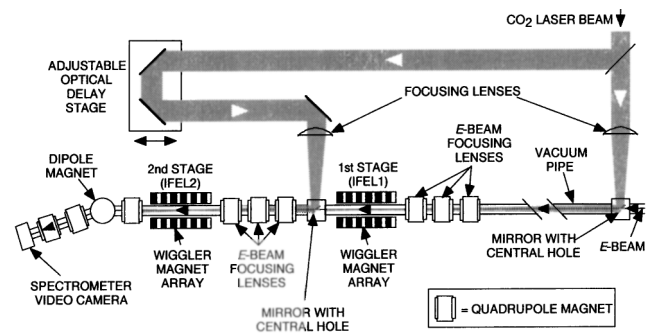

FIG. 1. Schematic layout for the STELLA experiment. For size reference, the distance separating the two IFELs is 2.3 m and the laser beams enter the beam line ≈6 m apart.

pipe, which have central holes for transmission of the *e*-beam. These mirrors direct the laser beams collinear to the *e*-beam. The annular laser beams are focused into modified Airy patterns inside the undulators. The center of this pattern closely matches the Gaussian shape of the *e*-beam inside the undulator.

In the first IFEL, the electrons experience uniform laser intensity because the 3-ps *e*-beam pulse is much shorter than the 180-ps laser pulse and narrower than the laser beam. However, since the laser wave oscillates with a period of 30 fs, the electrons experience varying amplitude and alternating polarity of the sinusoidal laser field, thereby resulting in some electrons being accelerated, some decelerated, and some with practically no energy change. This sinusoidal energy modulation process was first measured earlier during the STELLA program [10]. If these electrons are allowed to drift downstream, then the accelerated electrons catch up with the decelerated ones resulting in the formation of a train of microbunches spaced apart at the laser wave period. This basic process occurs routinely in microwave-driven accelerators; the complication in laser accelerators is that the bunch lengths and spacings are several orders of magnitude smaller.

Only ≈24 MW is sent to the first IFEL, which is the amount needed to achieve optimum microbunching at the second stage location. Most of the laser power (up to 300 MW) is transmitted to the second IFEL for acceleration.

An electron energy spectrometer at the end of the beam line detects the resulting time-integrated energy distribution of all the electrons in the *e*-beam, i.e., both electrons within and outside the microbunches. Figure 2 presents sample gray scale images from the spectrometer camera. Figure 2(a) shows the *e*-beam energy distribution with the laser off. The center and width of the line image corresponds to the mean energy and intrinsic energy spread of the *e*-beam, respectively. Figure 2(b) displays the sinusoidal energy modulation imparted by the first IFEL operating alone. Note how electrons are symmetrically accelerated and decelerated about the mean energy position.

Figures 2(c) and 2(d) demonstrate our ability to synchronize the microbunches created by the first IFEL to the laser field phase in the second IFEL. By adjusting the optical delay, the laser phase shifts by 180° and results in a transition from maximum acceleration [Fig. 2(c)] where a well-defined peak is observed at the positive edge of the image corresponding to the accelerated microbunches, to maximum deceleration of the microbunches [Fig. 2(d)] where the peak shifts to the left. This femtosecond phase control could be maintained over periods of many minutes before gradual phase drifts occurred. The long time constant of the drift should allow implementation of various feedback schemes to lock the phase for arbitrarily long periods.

More detailed information about this process can be obtained by comparing the energy spectra results with a model as shown in Fig. 3 for a near maximum acceleration case. Table I lists the parameters for the STELLA experiment and the values used in the model comparisons.

Our 3D computer model incorporates all essential factors including 1D longitudinal space-charge effects, *e*-beam emittance, and possible misalignment of the *e*-beam and laser beams along different parts of the beam line. [The last two entries in Table I (*e*-beam angular error and centroid offset) are values determined by iterating the model for best fit to the data. These quantities are within

(a)   (b)

(c)

FIG. 3.   Comparison of staging results with model for phase delay corresponding to near maximum acceleration. (a) Model-predicted electron output phase versus electron energy. (b) Model-predicted electron bunch length. (c) Electron energy spectrum predicted by model together with cross section from spectrometer video image.
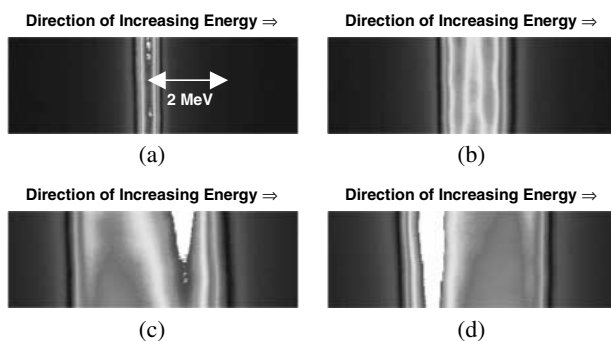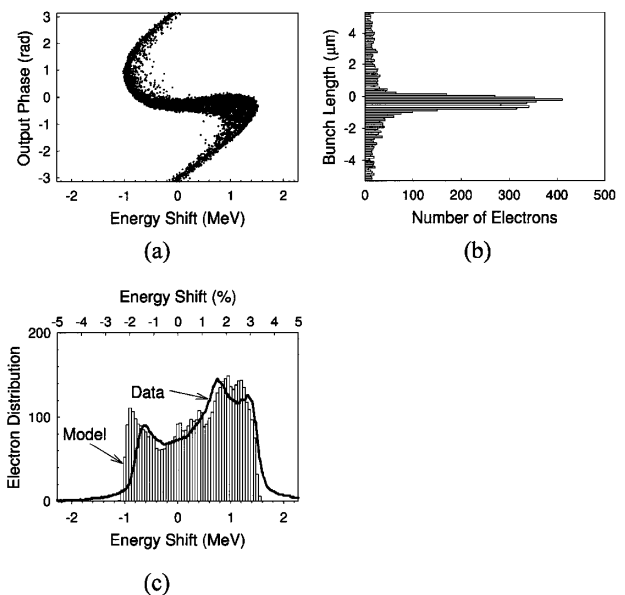

FIG. 2.   Raw video images (gray scale) from electron energy spectrometer for the conditions given in Table I. Energy dispersions is in the horizontal direction as shown; the vertical direction provides essentially redundant information. White is saturation. (a) Laser off to both IFELs. (b) Sinusoidal energy modulation from first IFEL only. (c) Lasers on to both IFELs. Phase delay set for maximum acceleration. (d) Same conditions as (c) with phase delay set 180° from (c).

TABLE I. STELLA experimental parameters and values used in model.

Parameter	Value
E-beam energy	45.6 MeV
E-beam intrinsic energy spread (1σ)	0.04%
E-beam charge (total pulse)	0.1 nC
E-beam pulse length (1σ)	≈ 3 ps
E-beam normalized emittance	1.5 mm mrad
Laser pulse length (FWHM)	≈ 180 ps
Laser wavelength (CO_2 laser)	10.6 μm
Laser polarization	Linear
Laser power to IFEL1	24 MW
Laser beam size inside IFEL1 (1σ)	0.67 mm
Laser power to IFEL2	200 MW
Laser beam size inside IFEL2 (1σ)	0.62 mm
E-beam angular error entering IFEL1	0.4 mrad in x and y
E-beam centroid offset entering IFEL1	0.7 mm in x only

the accuracy that the e-beam could be aligned into the first wiggler.]

Figure 3(a) shows a longitudinal phase-space plot where the coordinates are energy and phase measured relative to an arbitrary reference energy and phase. The phase-space plot can be projected onto either the phase axis [Fig. 3(b)], or the energy axis [Fig. 3(c)]. [Note, since 2π of the phase corresponds to 10.6 μm, Fig. 3(b) plots phase in the equivalent units of length.] The projection on the energy axis corresponds to the directly measurable e-beam energy spectrum. The simulation used 5000 electrons, and the model and data energy spectra are adjusted to have equal areas.

The model reveals characteristics about the electron behavior, which are not evident from the energy spectrum alone. In Fig. 3(b), the model predicts the bunch length is quite short [~ 0.8 μm (full width at half maximum) or ~ 2.7 fs]. While ~ 2–3 fs microbunches were first generated in earlier laser acceleration experiments at the AFT [11], during STELLA these short microbunches are measured for the first time in a direct manner by detecting their energy distribution from which their bunch length was inferred. This is also much shorter than recently reported direct detection of 100-fs microbunches [12].

Because of the short, untapered undulator used, less than one synchrotron oscillation occurs and the separation in energy of the microbunches from the nonaccelerated electrons is incomplete. This explains why the energy spread of the accelerated electrons ($\sim 2\%$) is relatively large for a practical accelerator. However, our model predicts that monoenergetic acceleration, with complete separation and energy spreads $<1\%$, will occur using a tapered undulator and higher laser power for the second IFEL.

Note that IFELs cannot reach the high acceleration gradients of some other laser acceleration methods; however, their inherent simplicity greatly eased the experimental difficulties of demonstrating staging. The experiment also showed the benefits of using a long wavelength laser, which eases stability and rephasing requirements, and lessens sensitivity to microbunch disruption effects.

Thus, STELLA has shown it is possible to resynchronize optically bunched electrons with a laser wave in a controlled manner. The importance of this is its general applicability to other more promising laser acceleration methods that have demonstrated much higher gradients [5] and have more favorable scaling potential. We believe this is a fundamental accomplishment that has addressed crucial system issues and will help spur the development of practical multistage, monoenergetic laser accelerators.

*Electronic address: wkimura@stioptronics.com

[1] J. People, Jr., in *Proceedings of the 1997 Particle Accelerator Conference, Vancouver, BC, 1997,* edited by M. Comyn *et al.,* (IEEE, New York, 1998), p. 29.

[2] W. H. Scharf and O. A. Chomicki, Phys. Medica **XII**, 199 (1996).

[3] See, for example, Nat. Struct. Biol. Synchrotron Suppl. **5** (1998); *Symposium Proceedings of the Applications of Synchrotron Radiation Techniques to Material Science,* edited by S. M. Mini *et al.,* (Materials Research Society, Warrendale, PA, 1998).

[4] M. J. Kelley *et al.,* SPIE **2703**, 15 (1996).

[5] W. P. Leemans and E. Esarey, in *Proceedings of Advanced Accelerator Concepts 8th Workshop, Baltimore, Maryland, 1998,* edited by W. Lawson, C. Bellamy, and D. Brosius, AIP Conf. Proc. No. 472 (AIP, New York, 1999), p. 174.

[6] I. V. Pogorelsky *et al.,* IEEE J. Quantum Electron. **31**, 556 (1995).

[7] W. D. Kimura *et al.,* in *Proceedings of Advanced Accelerator Concepts 8th Workshop, Baltimore, Maryland, 1998* (Ref. [5]), p. 563.

[8] K. P. Kusche *et al.,* in *Proceedings of Advanced Accelerator Concepts 8th Workshop, Baltimore, Maryland, 1998,* (Ref. [5]), p. 573.

[9] R. B. Palmer, J. Appl. Phys. **43**, 3014 (1972).

[10] L. P. Campbell *et al.,* IEEE Trans. Plasma Sci. **28**, 1143 (2000).

[11] Y. Liu *et al.,* Phys. Rev. Lett. **80**, 4418 (1998).

[12] K. N. Ricci and T. I. Smith, Phys. Rev. ST Accel. Beams **3**, 032801 (2000).